Mechanisms of the Reactions of W and W^+ with NO_x ($x = 1, 2$): A Computational Study

Hsin-Tsung Chen, Djamaladdin G. Musaev,* Stephan Irle,* and M. C. Lin*

Cherry L. Emerson Center for Scientific Computation and Department of Chemistry, Emory University, 1515 Dickey Drive, Atlanta, Georgia 30322

Received: November 2, 2006; In Final Form: December 11, 2006

The mechanisms of the reactions of W and W^+ with NO_x ($x = 1, 2$) were studied at the CCSD(T)/[SDD+6-311G(d)]//B3LYP/[SDD+6-31G(d)] level of theory. It was shown that the insertion pathway of the reaction $W(^7S) + NO_2(^2A_1)$ is a multistate process, which involves several lower lying electronic states of numerous intermediates and transition states, and leads to oxidation, $WO(^3\Sigma) + NO(^2\Pi)$, and/or nitration, $WN(^4\Sigma) + O_2(^3\Sigma_g^-)$, of the W-center. Oxidation products $WO(^3\Sigma) + NO(^2\Pi)$ lie 87.6 kcal/mol below the reactants, while the nitration channel is only 31.0 kcal/mol exothermic. Furthermore, it was shown that nitration of W with NO_2 is kinetically less favorable than its oxidation. The addition−dissociation pathway of the reaction $W(^7S) + NO_2(^2A_1)$ proceeds via the octet (ground) state potential energy surface of the reaction, requires 3.3 kcal/mol barrier, and leads exclusively to oxidation products. Calculations show that oxidation of the W^+ cation by NO_2 is a barrierless process in the gas phase, proceeds exclusively via the insertion pathway, and is exothermic by 82.9 kcal/mol. The nitration of W^+ by NO_2 is only 14.1 kcal/mol exothermic and could be accessible only under high-temperature conditions. Reactions of M = W/W^+ with NO are also barrierless processes in the gas phase and lead to the N−O insertion product NMO, which are 105.4 and 77.4 kcal/mol lower than the reactants for W and W^+, respectively.

I. Introduction

Understanding the mechanisms and factors governing the reactions of transition metal systems with small molecules (NO_x ($x = 1$ and 2), N_2, CO_x ($x = 1$ and 2), O_2, H_2O, hydrocarbons, etc.) is essential for designing novel and more efficient catalysts for important chemical processes, such as nitrogen fixation, hydrocarbon hydroxylation, utilization of carbon mono- and dioxides, and more. The mechanisms of these important reactions are usually affected by numerous factors including redox activity and spin states of transition metal centers, the nature of their ligand environment, the identity of reactive intermediates, and the nature of the substrate, solvent, and support materials. The first step toward elucidating the role of these various factors is to study the gas-phase reactions of transition metal (TM) atoms and ions with small molecules, since the gas-phase reactions are free from ligand, solvent, and support effects. Such studies can provide vital information on the role of the nature of transition metal centers and their lower lying electronic states in these reactions. In obtaining atomistic level understanding of these reactions, the computational approaches along with gas-phase experiments have proved to be very useful.[1,2] Indeed, state-of-the-art calculations of the potential energy surfaces (PESs) of these reactions on several low-lying electronic states of reactants, intermediates, and products can provide essential knowledge for interpretation of experimental results and for a comprehensive understanding of complicated mechanisms of the reactions involving TM systems.

This paper is a continuation of our previous efforts[3] and deals with the reaction of W and W^+ with NO_x ($x = 1$ and 2) molecules. As mentioned in the literature, tungsten and tungsten alloys are important materials widely used in high-temperature environments.[4] Therefore, the understanding of the reaction mechanisms of tungsten systems with combustion products has been the focus of many previous studies.[5]

To the best of our knowledge, the reactions of W^+ with NO_x ($x = 1, 2$) as well as W atom with NO_2 have not been investigated before. However, the reaction of W atom with NO was previously reported. Andrews and Zhou have reported[6] that laser-ablated W atoms react with NO to give primarily the nitric oxide insertion product NWO. Intermediate W(η^1-NO) and W(η^2-NO) were not observed, while complexes W(η^1-NO)$_n$ (where $n = 2$, 3, and 4) were observed. They also have reported density functional studies on the relative energies, structures, frequencies, and isotopic shift parameters of the WNO systems. Harter and co-workers[7] have reported the depletion kinetics of low-lying states of W atom in the presence of NO. On the other hand, the interaction of NO_2 with alkaline,[8−15] alkaline-earth,[16−20] and transition metals[20−25] have been extensively studied using both theoretical and experimental methods. The latter studies have demonstrated that the NO_2 molecule can coordinate to metal centers in several ways[26] (see Figure 1). The most stable isomer of MNO_2 is an M(η^2-O_2N) complex for the alkali and alkaline-earth metals (M = Li, Na, Be, Mg, Ca, and Sr). For the group 11 metals, this picture is slightly more complex: for M = Cu and Ag, the most stable isomer of MNO_2 is an M(η^2-O_2N) structure, while for M = Au, it is an M(η^1-ONO) structure.

Perhaps most similar to our present study of W/W^+ reactions with NO_x ($x = 1, 2$), Stirling[27] reported density functional studies of the reactions between NO_2 and Sc, Ti, and V atoms in their ground electronic states. It was shown that these reactions proceed smoothly via direct insertion of the metal atoms into an N−O bond with almost no barrier, leading to the OM−NO product. The calculated OM−NO binding energies, 81.8 (M = Sc), 92.1 (M = Ti), and 86.8 (M = V) kcal/mol, are in very

10.1021/jp067238f CCC: $37.00
Published on Web 01/18/2007

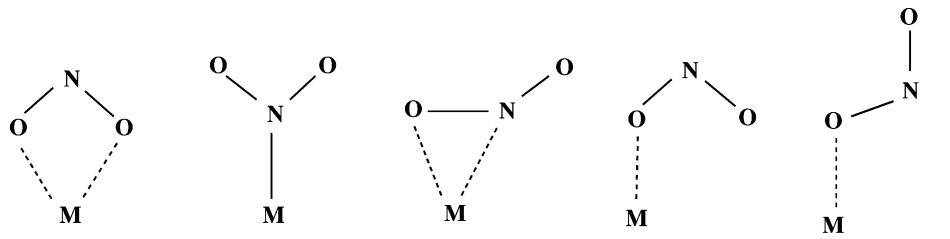

Figure 1. Possible isomers of the $M(NO_2)$ intermediate.

good agreement with their experimental values, 89.9 ± 2.7, 87.7 ± 2.2, and 76.8 ± 4.5 kcal/mol, respectively. Since W and W^+ chemistry involves several low-lying electronic states, we are including singlet, triplet, and quintet state surfaces for the reactions of W with NO_2, and doublet, quartet, and sextet state surfaces in the case of W^+, and we go beyond the first ON−metal−O insertion step.

II. Computational Procedures

The potential energy surfaces (PESs) of the reactions $W/W^+ + NO_x$ in several low-lying electronic states of W and W^+ were calculated using the Gaussian 03 quantum chemical software package.[28] The geometries of the reactants, intermediates, transition states, and products of these reactions were optimized without imposing symmetry constraints at the B3LYP density functional level.[29] In these calculations we used the Stuttgart/Dresden relativistic effective core potential (ECP)[30] and associated triple-ζ SDD basis set for W, and the 6-31G(d) basis set for main group elements. Below, we call this approach as B3LYP/[SDD+6-31G(d)]. The nature of all stationary points was confirmed by performing normal-mode analysis. In addition, the nature of the calculated transition states was clarified using the intrinsic reaction coordinate (IRC) approach.[31] Previously, it was demonstrated that the B3LYP method with double-ζ plus polarization basis sets provides an excellent agreement with experiments for geometries of transition metal systems.[32] However, B3LYP-calculated energies could be off their most accurate values by several kilocalories per mole. Therefore, we improved the energy of the calculated structures by performing single-point UCCSD(T) (for simplicity called below CCSD(T)) calculations at their B3LYP-optimized geometries. In the CCSD(T) calculations we extended the basis sets for main group elements from 6-31G(d) to 6-311G(d). Unscaled zero-point energy corrections (ZPC) estimated at the B3LYP level added to the final CCSD(T) energetics. The single-determinant nature of the wave function of all calculated structures was confirmed by performing T1 diagnostics (the T1 parameter for all structures is calculated to be within 0.01−0.06). We also checked the $\langle S^2 \rangle$ values to evaluate the spin contamination in these calculations. As seen from the materials (Tables S1 and S2) given in the Supporting Information, in general, spin contamination in these calculations is not significant. Throughout the paper we discuss the CCSD(T) energetics, while the B3LYP energetics (relative energies) are included in the Supporting Information.

As will be discussed below, PESs of several lower lying electronic states of the studied reactions cross many times upon completion. Search for the exact location of seam of crossing of these PESs would require the use of computationally much more demanding methods and inclusion of the spin−orbit-coupling (SOC) effect in the calculations. Because of technical limitations, in this paper, we did not perform SOC calculations and did not search for the seam of crossing of PESs of the lower lying electronic states of the studied reactions, following our previous computational methodology.[3]

TABLE 1: Comparison of Calculated and Experimental Values for Heats of Various Reactions Studied in This Paper (All Values in kcal/mol)

reaction	calcd	expt[a]
$W(^7S)/W^+(^6D) + NO_2(^2A_1) \rightarrow$		
$WO(^1\Sigma^+) + NO(^2\Pi)$	−64.3	
$WO(^3\Sigma^+) + NO(^2\Pi)$	−87.6	-100.6 ± 17
$WO^+(^2\Sigma^+) + NO(^2\Pi)$	−55.9	
$WO^+(^4\Sigma^+) + NO(^2\Pi)$	−82.9	-96.1 ± 23.9
$W(^7S)/W^+(^6D) + NO(^2\Pi) \rightarrow$		
$WO(^1\Sigma^+) + N(^4S)$	8.2	
$WO(^3\Sigma^+) + N(^4S)$	−15.1	-22.1 ± 17
$WO^+(^2\Sigma^+) + N(^4S)$	16.6	
$WO^+(^4\Sigma^+) + N(^4S)$	−11.9	-17.5 ± 23.9

[a] The experimental heats of reaction at 0 K for $W(^7S) + NO_2(^2A_1) \rightarrow WO(^1\Sigma^+ \text{ or } ^3\Sigma^+) + NO(^2\Pi)$, $W(^7S) + NO(^2\Pi) \rightarrow WO(^1\Sigma^+ \text{ or } ^3\Sigma^+) + N(^4S)$, $W^+(^6D) + NO_2(^2A_1) \rightarrow WO^+(^2\Sigma^+ \text{ or } ^4\Sigma^+) + NO(^2\Pi)$, and $W^+(^6D) + NO(^2\Pi) \rightarrow WO^+(^2\Sigma^+ \text{ or } ^4\Sigma^+) + N(^4S)$ are -100.6 ± 17, -96.1 ± 23.9, -22.1 ± 17, and -17.5 ± 23.9 kcal/mol, respectively, based on, $\Delta_f H_0(W) = 203.401$ kcal/mol,[33] $\Delta_f H_0(W^+) = 384.449$ kcal/mol,[34] $\Delta_f H_0(WO) = 90.136 \pm 17$ kcal/mol,[33b] $\Delta_f H_0(WO^+) = 275.767 \pm 23.9$ kcal/mol,[33b] $\Delta_f H_0(NO_2) = 8.85$ kcal/mol,[35] $\Delta_f H_0(NO) = 21.48$ kcal/mol,[36] and $\Delta_f H_0(N) = 112.64$ kcal/mol.[37]

III. Results and Discussion

As we discussed previously,[3] at the B3LYP and CCSD(T) levels of theory used in this paper, the ground electronic state of the W atom is calculated to be a septet ^7S state associated with the s^1d^5 electronic configuration, while the quintet ^5D state associated with the s^2d^4 electronic configuration is slightly, 4.6 kcal/mol, higher in energy (CCSD(T) data).These data are not consistent with that of Campbell-Miller and Simard, who have reported the ^5D ground electronic state for W atom.[33b] The calculated triplet ^3P (s^2d^4) and singlet ^1S (s^2d^4) states of W are calculated to be 45.0 and 71.5 kcal/mol higher in energy, respectively, at the CCSD(T)/[SDD+6-311G(d)] level of theory. Meanwhile, the ground electronic state of W^+ is the sextet ^6D state associated with the s^1d^4 electronic configuration: its quartet ^4F (s^1d^4) and doublet ^2P (s^1d^4) states are 27.6 and 47.0 kcal/mol higher in energies, which are in good agreement with 24.9 and 55.5 kcal/mol experimental values, respectively.[33a] The CCSD(T)-calculated ionization energy of $W(^7S)$ is 171.0 kcal/mol, which also is in reasonable agreement with the experimental value of 181.344 ± 0.002 kcal/mol.[33b] Furthermore, we have previously demonstrated that the computational approach used in this paper describes the heat of formation of diatomic molecules of W/W^+ with various ligands reasonably accurately.[3] In Table 1, we compare the available experimental data[33−37] with their calculated values for the heats of the reactions $W(^7S) + NO_2(^2A_1) \rightarrow WO(^1\Sigma^+ \text{ or } ^3\Sigma^+) + NO(^2\Pi)$, $W(^7S) + NO(^2\Pi) \rightarrow WO(^1\Sigma^+ \text{ or } ^3\Sigma^+) + N(^4S)$, $W^+(^6D) + NO_2(^2A_1) \rightarrow$

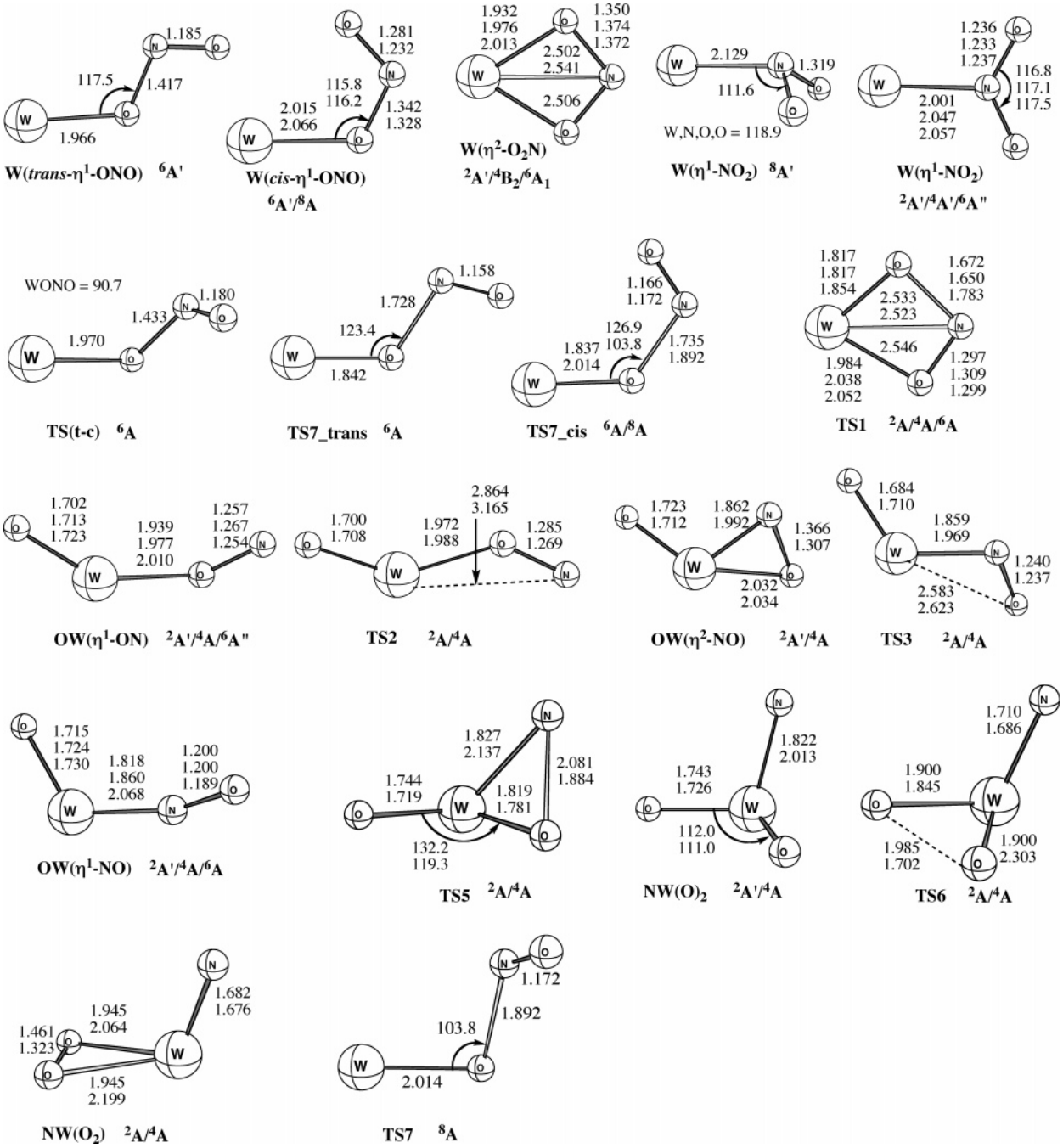

Figure 2. Optimized geometries of major intermediates, transition states, and products of the reaction of W with the NO_2 molecule. Distances are in angstroms, and angles are in degrees.

$WO^+(^2\Sigma^+$ or $^4\Sigma^+)$ + $NO(^2\Pi)$, and $W^+(^6D)$ + $NO(^2\Pi) \rightarrow$ $WO^+(^2\Sigma^+$ or $^4\Sigma^+)$ + $N(^4S)$. As seen from this table, the calculated values are in good agreement with the experimental data within the scatters.

Below, we present potential energy surfaces (PESs) of the reaction of NO_x with the ^7S, ^5D, ^3P, and ^1S spin states of the W atom, while the reaction of $W^+ + NO_x$ is investigated for the ^6D, ^4F, and ^2P states of W^+. The calculated structures of intermediates, transition states, and products of the reaction W + NO_2 are shown in Figure 2, while their energetics are presented in Figure 3. Those for the reaction $W^+ + NO_2$ are given in Figures 4 and 5, respectively. The calculated relative energies and $\langle S^2 \rangle$ values of the reactants, intermediates, transition states, and products of the reactions $W/W^+ + NO$ are given in Table 2.

III.1. Mechanism of the Reaction of W with NO_2. As shown in Figure 3a, this reaction may proceed via two different pathways, called the *insertion* and *addition*−*dissociation* pathways. The first step of both pathways is coordination of NO_2 to W. The resulting $W(NO_2)$ complex has several isomers, W(*cis*-η^1-ONO), W(*trans*-η^1-ONO), W(η^2-O_2N), and W(η^1-NO_2), as shown in Figure 2.

Calculations show that W(*trans*-η^1-ONO) is energetically the most favorable isomer, which is why direct insertion of W into the ON−O bond in analogy to reactions of Sc, Ti, and V with NO_2[22] are less likely. Its cis counterpart, W(*cis*-η^1-ONO), and isomers W(η^2-O_2N) and W(η^1-NO_2) lie 11.6, 25.8, and 18.3 kcal/mol higher in energy, respectively, than W(*trans*-η^1-ONO). The W(*cis*-η^1-ONO) isomer is separated from W(*trans*-η^1-ONO)

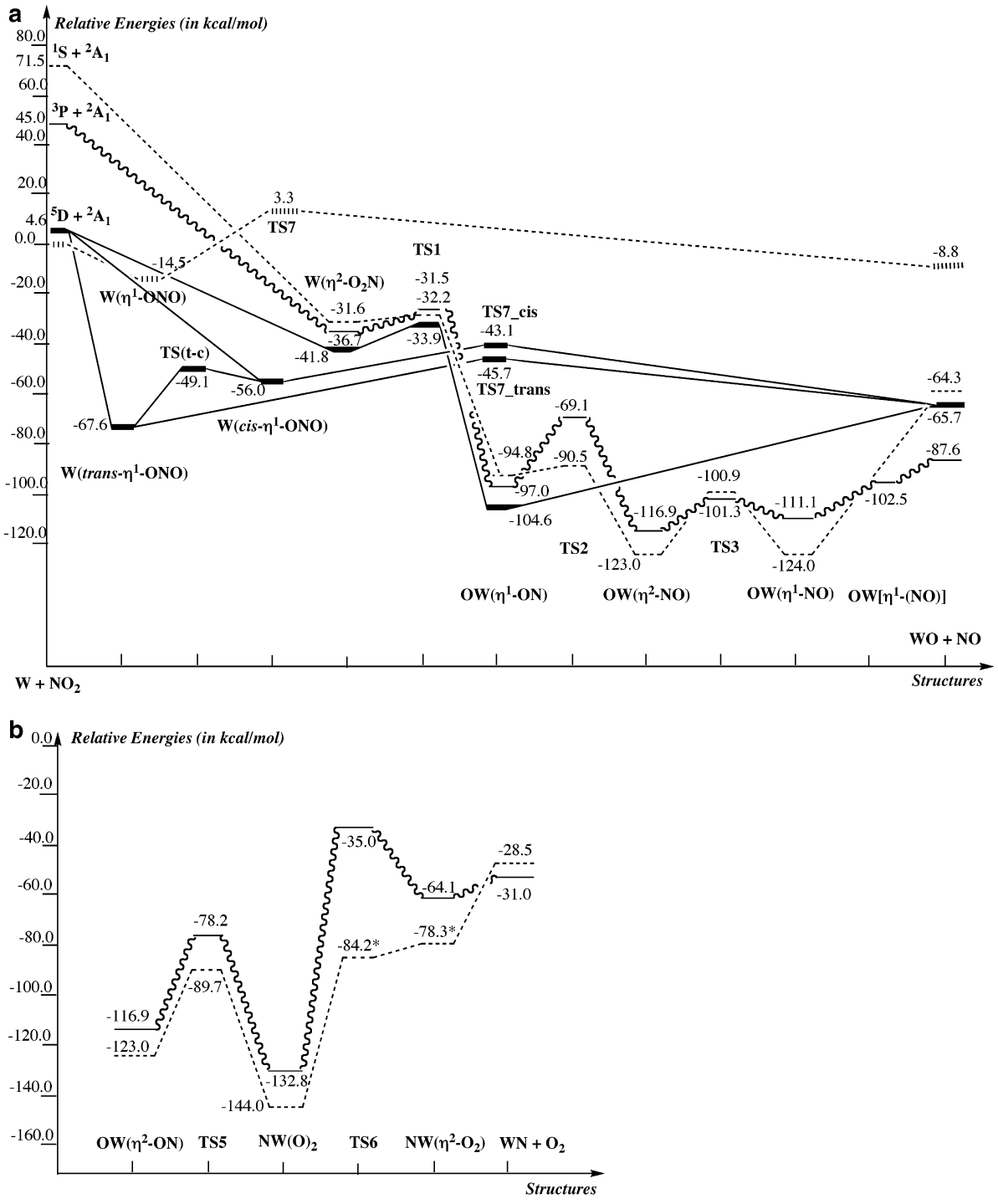

Figure 3. Calculated relative energies (in kcal/mol) of important intermediates, transition states, and products of the reaction of W with the NO_2 molecule. Calculated potential energy surfaces for (a) oxidation and (b) nitration of W by NO_2 on several low-lying electronic states of the reactants. *The B3LYP-calculated values are −78.1 and −90.4 kcal/mol for TS6 and NW(η^2-O_2), respectively.

by a 18.5 kcal/mol barrier (calculated from the most stable isomer) at the transition state TS(t-c).

The ground electronic state of the energetically most favorable W(*trans*-η^1-ONO) isomer is the sextet $^6A'$ state, which lies 67.6 kcal/mol lower than the W(^7S) + NO_2($^2A_1$) ground state reactants. The octet state of W(*trans*-η^1-ONO) lies 53.1 kcal/mol higher than the $^6A'$ ground state. In the doublet and quartet states the structure W(η^1-ONO) is not stable. The most stable electronic state of the W(η^2-O_2N) isomer is also the sextet state, which lies 41.8 kcal/mol lower than the W(^7S) + NO_2($^2A_1$) ground state reactants. Its doublet $^2A'$ and quartet $^4B_2$ states are higher in energy by 10.2 and 5.1 kcal/mol, respectively. At the octet state, W(η^2-O_2N) is not stable relative to ground state reactants. The doublet $^2A'$ and sextet $^6A''$ states of the W(η^1-NO_2) isomer are nearly degenerate with 49.3 and 48.9 kcal/mol energy relative to the ground state reactants. Its quartet and octet states are much higher in energy and will not be discussed.

The above presented results for the W(NO_2) complex are different from those for $CuNO_2$, $AgNO_2$, and $AuNO_2$ reported

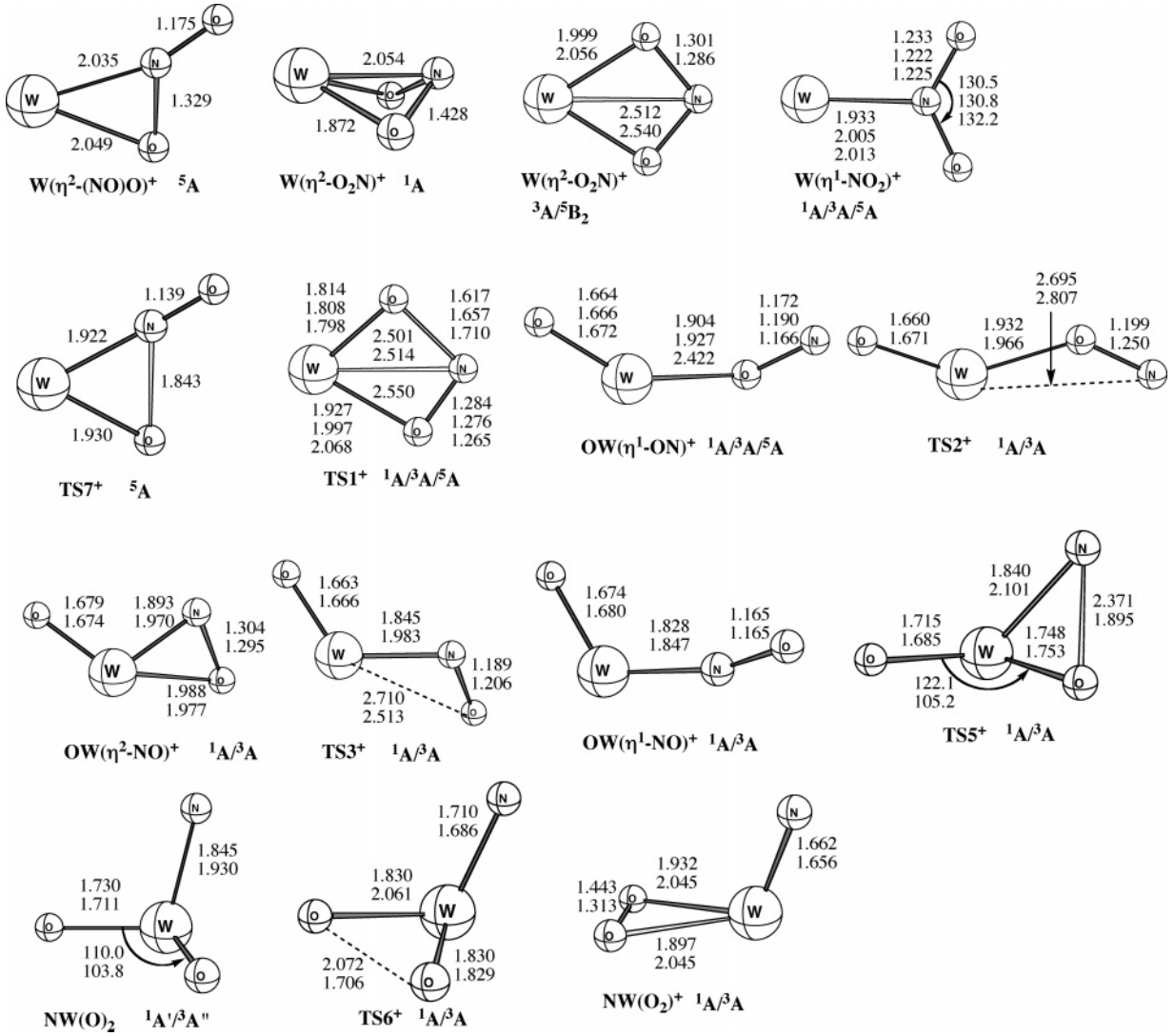

Figure 4. Optimized geometries of major intermediates, transition states, and products of the reaction of W^+ with the NO_2 molecule. Distances are in angstroms, and angles are in degrees.

in the literature: the most stable isomers of $CuNO_2$ and $AgNO_2$ correspond to the M(η^2-O_2N) structure, while for $AuNO_2$ it corresponds to the Au(*cis*-η^1-ONO) structure.[22,24] This could be partially explained by the fact that the third-row transition metals Au and W tend to provide a strong M−OCO bond compared to the Cu and Ag atoms.

Although we have calculated reaction pathways starting from all the located isomers of W(NO_2), we limit our discussions below mainly to the lower energy pathways. We mention the PESs of the high-energy pathways only when they cross the lower energy PESs and lead to more stable intermediates or products. We start our discussion with the insertion pathway.

As could be expected, from the energetically most favorable isomer W(*trans*-η^1-ONO)(^{6}A′), the reaction may proceed via three different pathways: (1) the activation of N−O bond and formation of OW−NO intermediate via a three-center transition state (involving W, N(O), and oxo fragments), (2) NO elimination, and (3) isomerization to its cis form.

All our efforts to locate a three-center N−O bond activation transition state, involving W, N(O), and oxo fragments, that could connect W(*trans*-η^1-ONO) and OW(η^1-NO) intermediates (via direct concerted pathway) were unsuccessful. Search for this transition state led either to TS7_trans (transition state for NO elimination, see below) or to the product OW(η^1-NO). Therefore, we conclude that a transition state connecting W(*trans*-η^1-ONO)(^{6}A′) to OW(η^1-NO)(^{2}A′) either does not exist or corresponds to seam of crossing of sextet and doublet PESs.

As seen in Figure 3a, the NO elimination from W(*trans*-η^1-ONO)(^{6}A′) proceeds with a 21.9 kcal/mol barrier at the transition state TS7_trans. The reaction W(*trans*-η^1-ONO)(^{6}A′) → WO($^5\Sigma^+$) + NO($^2\Pi$) is calculated to be endothermic by 1.9 kcal/mol.

At the next stage, the dissociated NO fragment may recoordinate to the W-center of the WO fragment to form the doublet OW(η^1-NO)(^{2}A′) complex. The formed OW(η^1-NO)(^{2}A′) complex lies 58.3 and 124.0 kcal/mol lower than WO($^5\Sigma^+$) + NO($^2\Pi$) and W(^{7}S) + NO_2($^2A_1$), respectively, and may rearrange to OW(η^2-NO)(^{2}A′) complex with about 23 kcal/mol barrier at the transition state TS3. Isomers OW(η^1-NO)(^{2}A′) and OW(η^2-NO)(^{2}A) are almost degenerate.

The formation of another linear isomer, OW(η^1-ON)(^{2}A′), from the cyclic OW(η^2-NO)(^{2}A′) is unlikely: OW(η^1-ON)(^{2}A′) → OW(η^2-NO)(^{2}A′) rearrangement requires a 32.5 kcal/mol barrier (at transition state TS2) and is endothermic by 18.4 kcal/mol.

However, this unfavorable OW(η^1-ON)(^{2}A′) intermediate could be formed via the W(*trans*-η^1-ONO)(^{6}A′) → W(*cis*-η^1-ONO)(^{6}A′) isomerization pathway. Indeed, as we mentioned above, trans → cis isomerization occurs with 18.5 kcal/mol (at the transition state TS(t-c)) and is endothermic by 11.6 kcal/

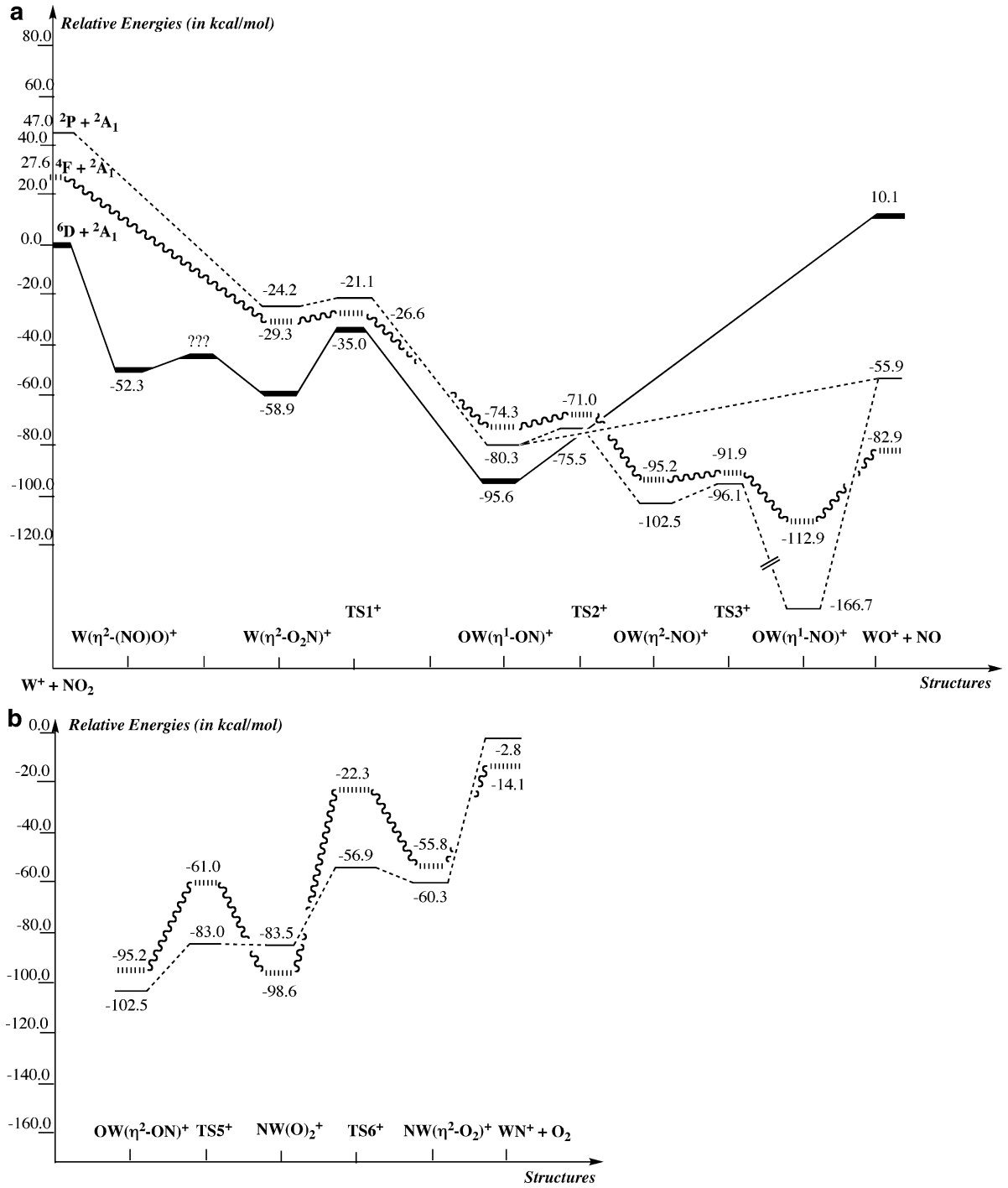

Figure 5. Calculated relative energies (in kcal/mol) of important intermediates, transition states, and products of the reaction of W^+ with the NO_2 molecule. Calculated potential energy surfaces for (a) oxidation and (b) nitration of W^+ by NO_2 on several low-lying electronic states of the reactants.

mol. From the resulting W(*cis*-η^1-ONO)(^{6}A′) reaction could proceed through (a) via NO elimination at the transition state TS7_cis, (b) via W(*cis*-η^1-ONO)(^{6}A′) → W(η^2-O_2N)(^{6}A$_1$) isomerization, and (c) or via sextet−quartet surface crossing that leads to formation of the OW(η^1-ON)(^{4}A) intermediate.

The NO elimination from the cis isomer (path a) occurs with a 12.9 kcal/mol barrier (calculated from W(*cis*-η^1-ONO)(^{6}A′)) at the transition state TS7_cis. After overcoming this transition state, the reaction follows via the pathway that was discussed for the W(*trans*-η^1-ONO)(^{6}A′) → OW(η^1-NO)(^{2}A′) rearrangement.

We have not been able to locate the transition state connecting W(*cis*-η^1-ONO)(^{6}A′) with W(η^2-O_2N)(^{6}A$_1$), path b. The calculated energy difference between these isomers of W(NO_2) complex, 14.2 kcal/mol, is larger than the NO-elimination barrier , 12.9 kcal/mol, at transition state TS7_cis. Therefore, it is unlikely that the W(*cis*-η^1-ONO)(^{6}A′) → W(η^2-O_2N)(^{6}A$_1$) isomerization (path b) could compete with the NO-elimination pathway (path a).

In contrast, path c could proceed via a lower barrier than path a. Indeed, as seen in Figure 3a, the sextet potential energy surface of NO elimination (path a) from W(*cis*-η^1-ONO)(^{6}A′) crosses the quartet surface of the W(η^2-O_2N)(^{4}B$_2$) → OW(η^1-ON)(^{4}A) reaction (path b) before (and/or below) transition state TS7_cis. As a result, the formation of OW(η^1-ON)(^{4}A) complex from W(*trans*-η^1-ONO)(^{6}A′) is expected to be feasible (which

TABLE 2: Calculated Relative Energies (in kcal/mol, Relative to the Ground State Reactants) of the Intermediates, Transition States, and Products of the Reactions M + NO for M = W and W^+ [a]

	W				W^+			
species	state	B3LYP ΔE + ZPE	CCSD(T) ΔE + ZPE	$\langle S^2\rangle$	state	B3LYP ΔE + ZPE	CCSD(T) ΔE + ZPE	$\langle S^2\rangle$
M + NO	^{1}S	68.31	71.47		^{2}D	49.05	47.00	0.89
	^{3}D	37.58	45.08	2.16	^{4}D	36.47	27.61	3.82
	^{5}D	5.21	4.61	6.19	^{6}D	0.00	0.00	8.75
	^{7}S	0.00	0.00	12				
M(η^1-NO)	$^2\Sigma_g$	−58.25	−46.27	0.8	$^1\Sigma_g$	−34.00	−36.51	0.00
	^{4}A″	−64.85	−47.47	3.97	$^3\Sigma_g$	−60.21	−40.67	2.08
	^{6}A″	−37.32	−25.29	8.78	$^5\Sigma_g$	−60.77	−46.82	6.12
	^{8}A″	−20.44	−11.34	15.76				
TS8	^{2}A′	−14.80	−11.69	2.05	^{1}A′	−0.24	14.29	0.00
	^{4}A″	−30.51	−14.31	4.83	^{3}A″	−31.65	−13.87	2.68
	^{6}A′	−7.56	4.46	8.78	^{5}A′	−33.03	−16.23	6.59
	^{8}A″	−6.48	0.46	15.76				
M(η^2-NO)	^{2}A′	−44.13	−33.10	0.86	^{1}A′	−25.08	−28.43	0.00
	^{4}A″	−49.98	−35.22	4.1	^{3}A′	−46.70	−29.84	2.38
	^{6}A″	−30.13	−14.99	8.78	^{5}A′	−46.50	−30.13	6.03
TS9	^{2}A′	−40.14	−29.65	0.78	^{1}A′	−26.46	−35.97	0.00
	^{4}A″	−38.13	−24.12	3.85	^{3}A′	−38.83	−23.44	2.11
	^{6}A′	5.33	16.52	8.83	^{5}A′	−5.97	12.88	6.05
NMO	^{2}A′	−118.94	−105.43	0.77	^{1}A′	−87.59	−77.36	0.00
	^{4}A″	−88.07	−76.52	3.76	^{3}A′	−85.59	−70.12	2.01
	^{6}A′	−51.85	−41.97	8.76	^{5}A′	−42.18	−26.98	6.01
M(η^1-ON)	^{2}A″	5.84	10.92	0.85	^{1}A	23.18	18.50	0.00
	$^4\Sigma_g$	−20.01	−5.81	5.11	$^3\Sigma_g$	−10.08	11.21	2.90
	^{6}A′	−9.29	1.49	8.78	^{5}A′	−27.76	−15.62	6.67
	^{8}A″	−14.69	−5.43	15.76				
MN + O	$^2\Sigma$	23.30	16.17	0.76	$^1\Sigma$	70.68	41.88	0.00
	$^4\Sigma$	12.87	13.65	3.81	$^3\Sigma$	31.13	30.63	2.03
	$^6\Sigma$	83.43	93.16	8.78	$^5\Sigma$	69.61	70.90	6.02
MO + N	$^1\Sigma^+$	12.06	8.24	0	$^2\Sigma^+$	26.91	16.62	0.76
	$^3\Sigma^+$	−7.30	−15.09	2.05	$^4\Sigma^+$	−8.67	−11.92	3.78
	$^5\Sigma^+$	10.50	6.80	6.02	$^6\Sigma^+$	83.05	82.67	8.75

[a] The $\langle S^2\rangle$ values of NO, N, and O are 0.75, 3.75 and 2.00, respectively.

could occur with less than 12 kcal/mol barrier). Later, the formed OW(η^1-ON)(^{4}A) complex rearranges to the most stable intermediates OW(η^2-NO)(^{2}A′) and OW(η^1-NO)(^{2}A′) with about 10 kcal/mol barrier required for a quartet−doublet seam of crossing.

Thus, the data presented above clearly show that in the gas phase the reaction W(^{7}S) + NO_2($^2A_1$) proceeds via the oxidation pathway W(*trans*-η^1-ONO)(^{6}A′) → W(*cis*-η^1-ONO)(^{6}A′) → OW(η^1-ON)(^{4}A) → OW(η^2-NO)(^{2}A′) → OW(η^1-NO)(^{2}A′) → WO···NO(^{4}A′) → WO($^3S^+$) + NO($^2\Pi$) and involves several lower lying electronic states of the reactants and intermediates. The overall oxidation reaction W(^{7}S) + NO_2($^2A_1$) → WO($^3S^+$) + NO($^2\Pi$) is calculated to be 87.6 kcal/mol exothermic.

We also followed the reaction pathway of the nitration W(^{7}S) + NO_2($^2A_1$) → W(*trans*-η^1-ONO)(^{6}A′) → W(*cis*-η^1-ONO)(^{6}A′) → OW(η^1-ON)(^{4}A) → OW(η^2-NO)(^{2}A′) → $NW(O)_2$(^{2}A′) → $NW(O_2)$(^{2}A) → WN($^4\Sigma^+$) + O_2($^3\Sigma_g^-$) (see Figure 3b). Our calculations show that the W nitration by NO_2 is 31.0 kcal/mol exothermic, which is much smaller than that of oxidation, 87.6 kcal/mol.

The first part of the nitration reaction, W(^{7}S) + NO_2($^2A_1$) → W(*trans*-η^1-ONO)(^{6}A′) → W(*cis*-η^1-ONO)(^{6}A′) → OW(η^1-ON)-(^{4}A) → OW(η^2-NO)(^{2}A′), is the same as for the oxidation process, discussed above. The intermediate OW(η^2-NO)(^{2}A′) is the splitting point of nitration and oxidation pathways. The nitration of W proceeds via a second N−O bond activation at the transition state TS5 and leads to formation of $NW(O)_2$(^{2}A′) intermediate, which lies 144 kcal/mol lower than the reactants. The intermediate $NW(O)_2$(^{2}A′) is the global minimum on the potential energy surface of the reaction W(^{7}S) + NO_2($^2A_1$). However, the formation of this intermediate from OW(η^2-NO)-(^{2}A′) is less feasible, because the rearrangement of OW(η^2-NO)-(^{2}A′) to OW(η^1-NO)(^{2}A′) that leads to oxidation of W occurs with ca. 11 kcal/mol lower barrier than the second N−O activation: OW(η^2-NO)(^{2}A) → TS5 → $NW(O)_2$(^{2}A′).

In summary, the data presented in Figure 3 indicate that the energetically and kinetically most favorable process on the insertion pathway of the reaction W(^{7}S) + NO_2($^2A_1$) is the oxidation of W leading to the WO($^3S^+$) + NO($^2\Pi$) products. However, we cannot fully exclude the nitration pathway leading to WN($^4\Sigma^+$) + O_2($^3\Sigma_g^-$), which occurs with a slightly larger barrier and is 51.6 kcal/mol less exothermic. The most stable intermediates on the PES of the reaction W(^{7}S) + NO_2($^2A_1$) are $NW(O)_2$(^{2}A′), OW(η^2-NO)(^{2}A′), OW(η^1-NO)(^{2}A′), and W(*trans*-η^1-ONO)(^{6}A′), which lie 144.0, 123.0, 124.0, and 67.6 kcal/mol lower than the ground state reactants.

Thus, the insertion pathway is a multistate process proceeding via numerous intermediates and transition states. All the located transition states and intermediates are lower in energy than the reactants.

As shown in Figure 3a, the reaction of W with NO_2 could also lead to the oxidation products WO + NO via the transition state TS7, without the formation of OWNO intermediates. We call this the addition−dissociation pathway, which follows via the octet, ground, state PES (i.e., W(^{7}S) + NO_2($^2A_1$)), forms the weakly (with a 14.5 kcal/mol binding energy) bound W(η^1-ONO)(^{8}A) intermediate, and requires only a 3.3 kcal/mol barrier (calculated relative to the W(^{7}S) + NO_2($^2A_1$) dissociation limit) in the gas phase. The product of this reaction WO($^7\Sigma^+$) + NO-($^2\Pi$) lies only 8.8 kcal/mol lower than the reactants and represents an electronically excited state of the insertion pathway products discussed above. The calculated barrier, 3.3 kcal/mol, for the addition−dissociation pathway is small, and we cannot

fully exclude the addition−dissociation mechanism for W oxidation by NO_2.

III.2. Mechanism of the Reaction of W^+ with NO_2. As shown in Figure 5a, one-electron ionization of the W-center effectively eliminates the addition−dissociation pathway for the reaction of W^+ with NO_2, which exclusively proceeds via an insertion mechanism. In addition, for the $W(NO_2)^+$ intermediate we could locate only two isomers: $W(\eta^2\text{-}(NO)O)^+$ and $W(\eta^2\text{-}O_2N)^+$ (see Figure 4). In the isomer $W(\eta^2\text{-}(NO)O)^+$, the NO_2 fragment coordinates to the W-center via its N−O bond, while in the isomer $W(\eta^2\text{-}O_2N)^+$ it coordinates via two O-centers. The ground state of both isomers is calculated to be a quintet ^5A state, which lies 52.3 and 58.9 kcal/mol lower than the ground state reactants $W^+(^6D) + NO_2(^2A_1)$, respectively. Since the isomer $W(\eta^2\text{-}(NO)O)^+$ easily rearranges to the thermodynamically most stable isomer $W(\eta^2\text{-}O_2N)^+$, below we only discuss the latter isomer, as well as the processes starting from it. Barriers separating these two isomers are very small, and we were not able to locate them.

Calculations show that the singlet and triplet states of $W(\eta^2\text{-}O_2N)^+$ are 37.8 and 29.5 kcal/mol higher in energy than the corresponding quintet ground state. In its quintet ground state, $W(\eta^2\text{-}O^2N)^+$ is quite stable and rearranges to the $OW(\eta^1\text{-}ON)^+$ intermediate with a 23.9 kcal/mol barrier at the transition state $TS1^+$. This transition state corresponds to the N−O bond activation and has an associated imaginary frequency of -596.2 cm^{-1}. The resulting $OW(\eta^1\text{-}ON)^+$ intermediate is calculated to be 95.6 and 36.7 kcal/mol lower in energy than $W^+(^6D) + NO_2(^2A_1)$ and $W(\eta^2\text{-}O_2N)^+(^5B_2)$, respectively.

From the intermediate $OW(\eta^1\text{-}ON)^+(^5A)$ the reaction, in general, may proceed via two different ways: (a) the dissociation of NO, leading to $WO^+(^6\Sigma^+) + NO(^2\Pi)$, and (b) the isomerization to $OW(\eta^2\text{-}NO)^+(^1A)$. The first process requires 105.7 kcal/mol and is not feasible. Meanwhile, the isomerization occurs with a relatively small barrier and proceeds via a quintet−singlet PES crossing. Although we did not locate the seam of quintet−singlet PES crossing, we expect it to lie below the singlet state transition state $TS2^+$. Therefore, the energy difference between $OW(\eta^1\text{-}ON)^+(^5A)$ and $TS2^+(^1A)$, 20.1 kcal/mol, can be taken as an upper limit of the barrier for $OW(\eta^1\text{-}ON)^+(^5A) \rightarrow OW(\eta^2\text{-}NO)^+(^1A)$ isomerization. This isomerization is exothermic by 6.9 kcal/mol.

From the resulting $OW(\eta^2\text{-}NO)^+(^1A)$ intermediate, the reaction may proceed via two distinct pathways: oxidation and nitration.

The oxidation pathway starts with the isomerization of $OW(\eta^2\text{-}NO)^+(^1A)$ to the thermodynamically most stable intermediate of the reaction $W^+(^6D) + NO_2(^2A_1)$, $OW(\eta^1\text{-}NO)^+(^1A)$. The calculated barrier for $OW(\eta^2\text{-}NO)^+(^1A) \rightarrow OW(\eta^1\text{-}NO)^+(^1A)$ rearrangement is 6.4 kcal/mol. The intermediate $OW(\eta^1\text{-}NO)^+(^1A)$ lies 166.7 and 64.2 kcal/mol below $W^+(^6D) + NO_2(^2A_1)$ and $OW(\eta^2\text{-}NO)^+(^1A)$, respectively. NO dissociation from $OW(\eta^1\text{-}NO)^+(^1A)$ leads to the oxidation product, $WO^+(^4\Sigma^+) + NO(^2\Pi)$, which occurs via a singlet−triplet seam of crossing. This product, $WO^+(^4\Sigma^+) + NO(^2\Pi)$, lies 82.9 kcal/mol lower than the ground state reactants, $W^+(^6D) + NO_2(^2A_1)$, but is in fact 83.8 kcal/mol higher in energy than the prereaction complex $OW(\eta^1\text{-}NO)^+(^1A)$.

The nitration of W requires (see Figure 5b) the second N−O bond activation, which occurs at $TS5^+$ with a 19.5 kcal/mol barrier. The product of the second N−O activation is the intermediate $NW(O)_2^+$, which is triplet in its ground state. The reaction $OW(\eta^2\text{-}NO)^+(^1A) \rightarrow NW(O)_2^+(^3A'')$ is calculated to be endothermic by 3.9 kcal/mol. The formation of the O−O bond and subsequent elimination of an O_2 molecule requires about 41.7 kcal/mol barrier (at the transition state $TS6^+$) and is endothermic by 84.5 kcal/mol. The nitration products $WN^+(^3\Sigma^+) + O_2(^3\Sigma_g^-)$ at their ground electronic states lie only 14.1 kcal/mol lower than $W^+(^6D) + NO_2(^2A_1)$.

Comparison of the above presented energetic for oxidation and nitration pathways clearly shows that the oxidation has generally lower barriers and is energetically the most accessible and feasible pathway.

In summary, our above presented findings clearly show that the reaction of W^+ with NO_2 occurs via an oxidation pathway and is exothermic by 82.9 kcal/mol. Since all calculated transition states are located below the reactants, one may expect that oxidation of W^+ by NO_2 is a barrierless process in the gas phase.

III.3. Mechanisms of the Reactions of W^+ and W with NO. In the following discussion we address only electronic ground state structures for all calculated intermediates, transition states, and products of the reaction $W/W^+ + NO$. The first intermediate of these reactions was expected to be an MNO (where M = W and W^+) structure, which may have three different isomers: $M(\eta^1\text{-}NO)$, $M(\eta^1\text{-}ON)$, and $M(\eta^2\text{-}NO)$ (presented in Table 2). Among these the isomer $M(\eta^1\text{-}NO)$ is found to be energetically the most favorable and lies by 47.5 and 46.8 kcal/mol below the reactants for M = W and M = W^+, respectively. The next stable isomer is a cyclic $M(\eta^2\text{-}NO)$, which lies by 12.3 and 16.7 kcal/mol higher than the corresponding $M(\eta^1\text{-}NO)$ isomer for M = W and M = W^+, respectively. Finally, the linear isomers $M(\eta^1\text{-}ON)$ are the least stable for both M = W and M = W^+. The barrier (at the transition state TS8) separating the *most* stable isomers $M(\eta^1\text{-}NO)$ from the cyclic isomers $M(\eta^2\text{-}NO)$ is high: 33.2 and 30.6 kcal/mol for M = W and M = W^+, respectively. In contrary, the barrier separating the *least* stable isomers $M(\eta^1\text{-}ON)$ from the cyclic isomers $M(\eta^2\text{-}NO)$ is only a few kilocalories per mole.

Calculations show that, for M = W and M = W^+, respectively, insertion of M into the N−O bond occurs with 17.8 and 10.8 kcal/mol (calculated from the corresponding $M(\eta^1\text{-}NO)$ intermediates) barriers (at the transition state TS9, see Table 2) and leads to the energetically most stable intermediates of the reactions M + NO, NMO structures, which are calculated to be 105.4 and 77.4 kcal/mol lower than the reactants. For M = W and M = W^+, respectively, the NMO intermediates are found to be 67.9 and 30.6 kcal/mol lower in energy than the corresponding $M(\eta^1\text{-}NO)$ intermediates.

Since reaction of W/W^+ with NO is highly exothermic and all calculated transition states lie below the reactants, we conclude that it occurs without barrier in the gas phase and leads to the most stable NWO product for both M = W and M = W^+. Our conclusion is in excellent agreement with the experimental data[6] of Andrews and Zhou, who showed that laser-ablated W atoms react with NO molecule to give primarily the nitrite oxide insertion product NWO.

The oxidation of W and W^+ by NO, i.e., the reactions M + NO → MO + N, is calculated to be exothermic by 15.1 and 13.7 kcal/mol, respectively, while the corresponding nitration reactions are found to be endothermic by 11.9 and 30.6 kcal/mol, respectively. The calculated 15.1 kcal/mol for the reaction W + NO → WO + N is in good agreement with the 10.5 kcal/mol experimental value reported by Harter and co-workers.[7]

IV. Conclusions

From the above presented discussion one can draw the following conclusions:

1. The reaction $W(^7S) + NO_2(^2A_1)$ could proceed via two distinct mechanisms, insertion and addition−dissociation, among which the insertion mechanism is energetically the most favorable one. The insertion pathway is a multistate process, proceeds via numerous intermediates and transition states, and leads to the oxidation of the W-center: $W(^7S) + NO_2(^2A_1) \rightarrow W(trans\text{-}\eta^1\text{-ONO})(^6A') \rightarrow W(cis\text{-}\eta^1\text{-ONO})(^6A') \rightarrow OW(\eta^1\text{-ON})(^4A) \rightarrow OW(\eta^2\text{-NO})(^2A') \rightarrow OW(\eta^1\text{-NO})(^2A') \rightarrow WO\cdots NO(^4A') \rightarrow WO(^3S^+) + NO(^2\Pi)$. All located transition states are lower in energy than the reactants. The oxidation reaction $W(^7S) + NO_2(^2A_1) \rightarrow WO(^3S^+) + NO(^2\Pi)$ is calculated to be 87.6 kcal/mol exothermic. However, we cannot fully exclude the nitration pathway leading to $WN(^4\Sigma^+) + O_2(^3\Sigma_g^-)$. It starts from the $OW(\eta^2\text{-NO})(^2A')$ intermediate, requires ca. 11 kcal/mol higher energy barrier than the $OW(\eta^2\text{-NO})(^2A') \rightarrow OW(\eta^1\text{-NO})(^2A')$ rearrangement located on the oxidation path, and is 51.6 kcal/mol less exothermic than the oxidation process, but is nevertheless feasible in the gas phase as all structures are below the energy of the reactants.

2. The addition−dissociation pathway exclusively leads to oxidation of W-centers, proceeds via the octet ground state PES of the $W(^7S) + NO_2(^2A_1)$ reaction, and requires a 3.3 kcal/mol barrier. The products $WO(^7\Sigma^+) + NO(^2\Pi)$ lie only 8.8 kcal/mol lower than the ground state reactants. The calculated barrier, 3.3 kcal/mol, for the addition−dissociation pathway is small, and one cannot fully exclude the addition−dissociation mechanism for W oxidation by NO_2.

3. The reaction of W^+ with NO_2 proceeds exclusively via the insertion pathway, $W^+(^6D) + NO_2(^2A_1) \rightarrow W((\eta^2\text{-}O_2N)^+(^5B_2) \rightarrow OW(\eta^1\text{-ON})^+(^5A) \rightarrow OW(\eta^2\text{-NO})^+(^3A) \rightarrow OW(\eta^1\text{-NO})^+(^3A) \rightarrow WO^+(^4\Sigma^+) + NO(^2\Pi)$, and is exothermic by 82.9 kcal/mol. Since all calculated transition states are located below the reactants, one may expect that the oxidation of W^+ by NO_2 is a barrierless process in the gas phase. The nitration of W^+ by NO_2 is only 14.1 kcal/mol exothermic and is the energetically least favorable pathway for the reaction W^+ with NO_2, although it could be accessible at high temperatures.

4. The reaction of $M = W/W^+$ with NO leads to the NMO product, and is exothermic by 105.4 and 77.4 kcal/mol for W and W^+, respectively. Since all calculated transition states of the reaction M + NO lie below the reactants, one can conclude that the reaction of M with NO occurs without barrier in the gas phase for both $M = W$ and $M = W^+$ and leads to enegetically the most favorable product NMO. Our conclusion is in excellent agreement with the experimental data[6] shown that laser-ablated W atoms react with NO molecule to give primarily the nitrite oxide insertion product NWO.

Acknowledgment. We gratefully acknowledge (1) financial support from the Office of Naval Research under a MURI grant (Prime Award No. N00014-04-1-0683 and Subaward No. 2794-EU-ONR-0683), and (2) the Emerson Center for the use of its resources.

Supporting Information Available: Complete ref 28; Table S1, the B3LYP and CCSD(T) calculated relative energies (in kcal/mol, relative to the ground state reactants) of the intermediates, transition states, and products of the reactions $W + NO_2$ for several low-lying electronic states; Table S2, the B3LYP and CCSD(T) calculated relative energies (in kcal/mol, relative to the ground state reactants) of the intermediates, transition states, and products of the reactions $W^+ + NO_2$ for several low-lying electronic states; Table S3, Cartesian coordinates (in Å) of all reported structures in this paper. This material is available free of charge via the Internet at http://pubs.acs.org.

References and Notes

(1) (a) Musaev, D. G.; Koga, N.; Morokuma, K. *J. Phys. Chem.* **1993**, *97*, 4064. (b) Musaev, D. G.; Morokuma, K. *Isr. J. Chem.* **1993**, *33*, 307. (c) Musaev, D. G.; Morokuma, K.; Koga, N.; Nguyen, K. A.; Gordon, M. S.; Cundari, T. R. *J. Phys. Chem.* **1993**, *97*, 11435. (d) Musaev, D. G.; Morokuma, K. *J. Chem. Phys.* **1994**, *101*, 10697. (e) Musaev, D. G.; Morokuma, K. *J. Phys. Chem.* **1996**, *100*, 11600. (f) Perry, J. K.; Ohanessian, G.; Goddard, W. A., III. *J. Phys. Chem.* **1993**, *97*, 5238. (g) Perry, J. K.; Ohanessian, G.; Goddard, W. A., III. *Organometallics* **1994**, *13*, 1870. (h) Blomberg, M. R. A.; Siegbahn, P. E. M.; Svensson, M. *J. Phys. Chem.* **1994**, *98*, 2062. (i) Siegbahn, P. E. M.; Blomberg, M. R. A.; Svensson, M. *J. Am. Chem. Soc.* **1993**, *115*, 4191. (j) Michelini, M. C.; Russo, N.; Sicilia, E. *Inorg. Chem.* **2004**, *43*, 4944. (k) Chiodo, S.; Kondakova, O.; Michelini, M. C.; Russo, N.; Sicilia, E.; Irigoras, A.; Ugalde, J. M. *J. Phys. Chem. A* **2004**, *108*, 1069. (l) Michelini, M. C.; Sicilia, E.; Russo, N.; Alikhani, M. E.; Silvi, B. *J. Phys. Chem. A* **2003**, *107*, 4862. (m) Michelini, M. C.; Russo, N.; Sicilia, E. *J. Phys. Chem. A* **2002**, *106*, 8937. (n) Sicilia, E.; Russo, N. *J. Am. Chem. Soc.* **2002**, *124*, 1471.

(2) (a) In: *Structure/Reactivity and Thermochemistry of Ions*; Ausloos, P., Lias, S. G., Eds.; Reidel: Dordrecht, The Netherlands, 1987. (b) In: *Gas Phase Inorganic Chemistry*; Russell, D. H., Ed.; Plenum: New York, 1989. (c) *Selective Hydrocarbon Activation: Principles and Progress*; Davies, J. A., Watson, P. L., Liebman, J. F., Greenberg, A., Eds.; VCH: New York, 1990. (d) Eller, K.; Schwarz, H. *Chem. Rev.* **1991**, *91*, 1121. (e) In: *Gas-Phase Metal Reactions*; Fontijn, A., Ed.; Elsevier: Amsterdam, 1992. (f) Weisshaar, J. C. In: *Advances in Chemical Physics*; Ng, C., Ed.; Wiley-Interscience: New York, 1992; Vol. 81. (g) In: *Transition Metal Hydrides*; Dedieu, A., Ed.; VCH: New York, 1992. (h) In: *Bonding Energetics in Organometallic Compounds*; Marks, T. J., Ed.; ACS Symposium Series 428; American Chemical Society: Washington, DC, 1990; p 55. (i) Armentrout, P. B. In: *Gas Phase Inorganic Chemistry*; Russell, D. H., Ed.; Plenum: New York, 1989; p 1. (j) Armentrout, P. B.; Beauchamp, J. L. *Acc. Chem. Res.* **1989**, *22*, 315. (k) Armentrout, P. B. *Science* **1991**, *251*, 175. (l) Roth, L. M.; Freiser, B. S. *Mass Spectrometry Rev.* **1991**, *10*, 303. (m) Weisshaar, J. C. *Acc. Chem. Res.* **1993**, *26*, 213. (n) Irikura, K. K.; Beauchamp, J. L. *J. Am. Chem. Soc.* **1989**, *111*, 75. (o) Irikura, K. K.; Beauchamp, J. L. *J. Phys. Chem.* **1991**, *95*, 8344. (p) Schroder, D.; Schwarz, H. *Angew. Chem., Int. Ed. Engl.* **1995**, *34*, 1973, and references therein. (q) Haynes, C. L.; Chen, Y. M.; Armentrout, P. B. *J. Phys. Chem.* **1995**, *99*, 9110. (r) Chen, Y. M.; Armentrout, P. B. *J. Phys. Chem.* **1995**, *99*, 10775. (s) Bushnell, J. E.; Kemper, P. R.; Maitre, P.; Bowers, M. T. *J. Am. Chem. Soc.* **1994**, *116*, 9710. (t) van Koppen, P. A. M.; Kemper, P. R.; Bushnell, J. E.; Bowers, M. T. *J. Am. Chem. Soc.* **1995**, *117*, 2098. (u) Guo, B. C.; Castleman, A. W., Jr. *J. Am. Chem. Soc.* **1992**, *114*, 6152. (v) Guo, B. C.; Kerns, K. P.; Castleman, A. W., Jr. *J. Phys. Chem.* **1992**, *96*, 4879.

(3) Musaev, D. G.; Xu, S.; Irle, S.; Lin, M. C. *J. Phys. Chem. A* **2006**, *110*, 4495−4501.

(4) Song, G. M.; Wang, Y. J.; Zhou, Y. *Int. J. Refract. Met. Hard Mater.* **2003**, *21*, 1.

(5) Andrews, L.; Zhou, M. *J. Phys. Chem. A* **1999**, *103*, 4167−4173.

(6) Harter, J. S. S.; Campbell, M. L.; McClean, R. E. *Int. J. Chem. Kinet.* **1997**, *29*, 367−375.

(7) (a) Tamura, T.; Hamamura, T. *Bull. Chem. Soc. Jpn.* **1976**, *49*, 1780. (b) Tamura, T.; Hamamura, T. *Shinku* **1980**, *23*, 425. (c) Hamamura, T.; Tamura, T. *Shinku* **1982**, *25*, 98. (d) Hamamura, T.; Tamura, T.; Nakazawa, Y.; Inoue, K. *Shinku* **1985**, *28*, 289.

(8) Herm, R: R.; Herschbach, D. R. *J. Chem. Phys.* **1970**, *52*, 5783.

(9) Ham, D. O.; Kinsey, J. L. *J. Chem. Phys.* **1970**, *53*, 285.

(10) Milligan, D. E.; Jacox, M. E. *J. Chem. Phys.* **1971**, *55*, 3404.

(11) Goddard, J. D.; Klein, M. L. *Phys. Rev. A* **1983**, *28*, 1141.

(12) Barbeschi, M.; Bencivenni, L.; Ramondo, F. *Chem. Phys.* **1987**, *112*, 387.

(13) Ramondo, F. *Chem. Phys. Lett.* **1989**, *156*, 346.

(14) Ramondo, F.; Bencivenni, L.; Sanna, N.; Nunziante Cesaro, S. *J. Mol. Struct. (THEOCHEM)* **1992**, *253*, 121.

(15) Lo, W.-J.; Shen, M.-y.; Yu, C.-h.; Lee, Y.-P. *J. Chem. Phys.* **1996**, *104*, 935.

(16) Herm, R. R.; Lin, S. M.; Mims, C. A. *J. Phys. Chem.* **1973**, *77*, 2931.

(17) Tevault, E.; Andrews, L. *Chem. Phys. Lett.* **1977**, *48*, 103.

(18) Davis, H. F.; Suits, A. G.; Lee, Y. T. *J. Chem. Phys.* **1992**, *96*, 6710.

(19) Cheong, B. S.; Parson, J. M. *J. Chem. Phys.* **1994**, *100*, 2637.

(20) Rodríguez-Santiago, L.; Sodupe, M.; Branchadell, V. *J. Phys. Chem.* **1998**, *102*, 630.

(21) Worden, D.; Ball, D. W. *J. Phys. Chem.* **1992**, *96*, 7167.

(22) Vinckier, C.; Verhaeghe, T.; Vanhees, I. *J. Chem. Soc., Faraday Trans.* **1994**, *90*, 2003.

(23) Rodríguez-Santiago, L.; Branchadell, V.; Sodupe, M. *J. Chem. Phys.* **1995**, *103*, 9738.

(24) Rodríguez-Santiago, L.; Sodupe, M.; Branchadell, V. *J. Chem. Phys.* **1996**, *105*, 9966.

(25) Lu, X.; Xu, X.;Wang, N.; Zhang, Q. *J. Phys. Chem. A* **1999**, *103*, 10969.

(26) Hitchman, M. A.; Rowbottom, G. L. *Coord. Chem. Rev.* **1982**, *42*, 55.

(27) Stirling, A. *Chem. Phys. Lett.* **1998**, *298*, 101.

(28) Frisch, M. J.; et al. *Gaussian 03*, rev. C1; Gaussian, Inc.: Pittsburgh, PA, 2003.

(29) (a) Becke, A. D. *Phys. Rev. A* **1988**, *38*, 3098. (b) Lee, C.; Yang, W.; Parr, R. G. *Phys. Rev. B* **1988**, *37*, 785. (c) Becke, A. D. *J. Chem. Phys.* **1993**, *98*, 5648.

(30) (a) Schwerdtfeger, P.; Dolg, M.; Schwarz, W. H.; Bowmaker, G. A.; Boyd, P. D. W. *J. Chem. Phys.* **1989**, *91*, 1762. (b) Andrae, D.; Haubermann, U.; Dolg, M.; Stoll, H.; Preuss, H. *Theor. Chim. Acta* **1990**, *77*, 123. (c) Bergner, A.; Dolg, M.; KŸchle, W.; Stoll, H.; Preuss, H. *Mol. Phys.* **1993**, *80*, 1431.

(31) Fukui, K. *Acc. Chem. Res.* **1981**, *14*, 363.

(32) Moreria, I. de P. R.; Illas, F.; Martin, R. L. *Phys. Rev. B* **2002**, *65*, 155102, and references therein.

(33) (a) Moore, C. E. *Atomic Energy Levels*; NSRD-NBS, U.S.A.; U.S. Goverment Printing Office: Washington, DC, 1991; Vol. 1. (b) Campbell-Miller, M. D.; Simard, B. *J. Opt. Soc. Am. B* **1996**, *13*, 2115.

(34) Chase, M. W., Jr. NIST-JANAF Thermchemical Tables, Fourth Edition. *J. Phys. Chem. Ref. Data, Monogr.* **1998**, No. 9, 1.

(35) Blagojevic, V.; Koyanagi, G. K.; Lavrov, V. V.; Orlova, G.; Bohme, D. K. *Chem. Phys. Lett.* **2004**, *389*, 303.

(36) Gurvich, L. V.; Veyts, I. V.; Alcock, C. B. *Thermodynamic Properties of Individual Substances*, 4th ed.; Hemisphere: New York, 1989.

(37) Chase, M. W., Jr.; Davies, C. A.; Downey, J. R., Jr.; Frurip, D. J.; McDonald, R. A.; Syverud, A. N. JANAF Thermochemical Tables (Third Edition). *J. Phys. Chem. Ref. Data, Suppl.* **1985**, *14* (1), 1.